International Journal of Mass Spectrometry 313 (2012) 58–67

Contents lists available at SciVerse ScienceDirect

International Journal of Mass Spectrometry

journal homepage: www.elsevier.com/locate/ijms

Electrospray tandem mass spectrometry combined with authentic compound synthesis for structural characterization of an octamethylcyclotetrasiloxane plasma polymer

Thierry Fouquet[a,b], Julien Petersen[b], Joao A.S. Bomfim[b], Jérôme Bour[b], Fabio Ziarelli[c], David Ruch[b], Laurence Charles[a,*]

[a] Aix-Marseille Univ – CNRS, UMR 7273, Institut de Chimie Radicalaire, Spectrométries Appliquées à la Chimie Structurale, 13397 Marseille, France
[b] Department of Advanced Materials and Structures, Centre de Recherche Public Henri Tudor (CRPHT), 4002 Esch sur Alzette, Luxembourg
[c] Aix-Marseille Univ – CNRS, Fédération des Sciences Chimiques, Spectropole, FR1739, F-13397 Marseille, France

ARTICLE INFO

Article history:
Received 30 November 2011
Received in revised form 11 January 2012
Accepted 11 January 2012
Available online 21 January 2012

Keywords:
Plasma polymer
Tandem mass spectrometry
Structural characterization
Polysiloxane
Synthetic polymer

ABSTRACT

Electrospray tandem mass spectrometry was used here to study the soluble part of a thin film prepared by plasma polymerization of octamethylcyclotetrasiloxane (D4). Accurate mass measurements and ^{29}Si nuclear magnetic resonance (NMR) spectroscopy, as well as synthesis of authentic compounds used as models to understand the MS/MS behavior of plasma polymers, were combined to structurally investigate oligomers present in this extract. All precursor ions were protonated or ammoniated molecules, known to provide more useful information for dimethylsiloxane (DMS)-based polymers as compared to alkali adducts. Apart from a major compound consisting of two D4 units connected *via* an oxygen bridge, it was found that the soluble part of this plasma polymer was mainly composed of cyclolinear polysiloxanes, in which cyclic units composed of four DMS were covalently connected by linear DMS segments. As the size of precursor ions increases, discrepancies observed between MS/MS data of synthesized molecules and of plasma oligomers would reveal the presence of branched isomers in the soluble part of the film, consistently with the expected propensity of the plasma polymerization process to favor random branching.

1. Introduction

As defined by Biederman [1], the term "plasma polymer" denotes a material that is created as a result of a passage of an organic gas or vapor through an electric discharge. It is usually deposited as a thin, poorly soluble and highly cross-linked film. Due to their unique properties arising from their particular network organization, plasma polymers have a huge potential for industrial applications. In particular, organosilicon plasma polymer coatings formed from plasma polymerization of hexamethyldisiloxane (HMDSO) have been found to be good candidates for a wide range of applications such as gas barrier [2–4] and anticorrosion [5,6] coatings. The possibility of synthesizing and depositing such materials by atmospheric pressure plasma processes allows the use of low cost equipments which can be extended to on-line processing at industrial scale. Among various techniques enabling atmospheric pressure non thermal plasmas, dielectric barrier discharges (DBDs) consist of generating discharges in the gas gap between two plane-parallel metal electrodes, one of them being covered with a dielectric layer [7]. The plasma polymerization process is usually considered as a mechanism involving free radicals generated during collisions of energetic electrons with organic molecules injected in the gas gap [1]. As a result, plasma polymers are expected to be composed of short chains, randomly branched and terminated with a high degree of cross-linking, that is, a much more complex structure than that of materials synthesized by conventional polymerization methods.

Microstructural characterization of polymeric materials is the first step towards the understanding of their properties as well as a deeper knowledge of polymerization processes involved in their synthesis. Plasma polymers of HMDSO (ppHMDSO) were reported to consist of a mixture of both organic polydimethylsiloxane (PDMS) and inorganic (SiO_x) silica-based species, as revealed by conventional techniques such as Fourier Transform InfraRed (FTIR) spectroscopy [8–11] and X-ray photoelectron spectroscopy (XPS) [8]. Although these techniques are of asset for determining the nature of functional groups present in the plasma polymer film, they provide information on chemical composition rather than molecular structure. Alternatively, mass spectrometry is increasingly used for structural characterization of synthetic (co)polymers

* Corresponding author. Tel.: +33 491 28 8678; fax: +33 491 28 2897.
E-mail address: laurence.charles@univ-provence.fr (L. Charles).

1387-3806/$ – see front matter © 2012 Elsevier B.V. All rights reserved.
doi:10.1016/j.ijms.2012.01.007

[12], allowing mass measurement of monomers in MS analysis and structural information by performing tandem mass spectrometric experiments, where intact cationic adducts of polymers are activated and their dissociation products analyzed based on fragmentation rules established for reference polymers with the same skeleton [13]. However, the lack of appropriate chemical standards to understand MS/MS data obtained from plasma polymers prevents any reliable structural features to be proposed.

In order to establish a methodology to structurally characterize plasma polymers by mass spectrometry, a less complex material as compared to ppHMDSO was prepared by injecting a cyclic monomer composed of four dimethylsiloxane (DMS) units in the DBD device. This octamethylcyclotetrasiloxane, so-called D4 according to the nomenclature used for silicon-containing compounds (*vide infra*), is often reported as a final degradation product of polysiloxane pyrolysis [14–17]. It is thus expected to exhibit a higher stability in the plasma, as compared to HMDSO, and hence to limit the variety of reacting radical species in the plasma, giving rise to the production of less complex structures.

2. Experimental

2.1. Chemicals

Methanol was purchased from SDS (Peypin, France), tetrahydrofuran (THF) from Riëdel-de Haen (Seelze, Germany) while *n*-pentane (95%) was from Carl Roth (Karlsruhe, Germany). α,ω-Dihydroxy-terminated poly(dimethylsiloxane) (M_n 590 g mol^{-1}), D4 and ammonium acetate were from Sigma–Aldrich (St. Louis, MO) while acetoxyheptamethylcyclotetrasiloxane D4(Ac) was from Gelest (Morrisville, PA). Diisopropylethylamine (99.5%) as well as chlorotrimethylsilane (98%) purchased from Acros Organics (Geel, Belgium). Ultra-pure water was produced by a Milli-Q system (Millipore, Molsheim, France). All chemicals were used as received without further purification. Nitrogen (99.999%) used in the plasma polymerization process was from Air Liquide (Paris, France).

2.2. Plasma polymer synthesis

The plasma-polymerized films were deposited using a semi-dynamic dielectric barrier discharge (DBD) reactor at open atmosphere described in previous studies [5,18] and illustrated by Supplementary Fig. S1. The DBD discharge was generated between an earthed bottom aluminium plate and two high-voltage aluminum top plates with a surface of 300.08 cm^2 (34.1 cm × 8.8 cm for one electrode) protected by a glass plate which serves as a dielectric barrier. The gap between the electrodes was set to 1.5 mm. Deposition by nitrogen filamentary plasma discharge was carried out at atmospheric pressure and at room temperature. For the coating process, plasma discharges were generated by an AC power supply. The frequency was set to 6 kHz and the voltage was a sinusoid as a function of time. For each deposition, electrical discharge was of about 20 kV, which corresponded to a power density over the electrodes of 0.84 W cm^{-2}. During the experiment, the top electrode block moved over the sample at a constant speed (0.07 m s^{-1}). For each sample, the plasma coating consisted of 80 passes, leading to the formation of a film with a 300–350 nm thickness as measured by ellipsometry. The silicon substrates were positioned at the bottom electrode. The carrier gas flow, composed only of N_2, was set at 0.8 L s^{-1}. Octamethylcyclotetrasiloxane monomers were sprayed in a TSI 3076 nebulizing chamber at a 0.1 L s^{-1} flow rate, and injected into the gas before entering the plasma zone. The gas mixture containing the precursor aerosol was injected into the plasma through a slit between the two top electrodes.

2.3. Synthesis of authentic compounds

A typical procedure for the synthesis of targeted authentic compounds is detailed elsewhere [19] and will only be briefly described here (Scheme 1).

For D3T2D3 or D3TD$_m$TD3, using a Shlenk flask preliminary dried and kept under inert atmosphere, 2.0 g (5.9 mmol) of commercial (D4(Ac)) were reacted with 0.10 g (5.9 mmol) of water in the case of D3T2D3, or 1.6 g (2.9 mmol) of commercial linear hydroxy terminated PDMS (further noted OH-PDMS) in the case of D3TD$_m$TD3, in the presence of 0.76 g (5.9 mmol) of diisopropylethylamine (DIPEA) overnight at room temperature. To remove salt and residual amine, the mixture was dissolved in pentane and washed with deionized water several times. *n*-Pentane was finally evaporated with a rotary evaporator under vacuum to give a low-viscosity oily siloxane. The yield was 1.54 g (90%) for D3T2D3 and 2.0 g (86%) for D3TD$_m$TD3. For the synthesis of D3TD$_{m-1}$M, following the same preliminary preparation of the Schlenk flask as described above, 0.32 g (2.9 mmol) of chlorotrimethylsilane was added dropwise to a mixture of 1.6 g (2.9 mmol) of commercial linear OH-PDMS and 0.76 g (5.9 mmol) of DIPEA. The mono-capping reaction by chlorotrimethylsilane is considered to be complete after the addition of all reactants but the product was not isolated; 1.0 g (2.9 mmol) of D4(Ac) was then added to the mixture directly after and allowed to react overnight at room temperature. The mixture was finally dissolved in *n*-pentane, washed with deionized water and the solvent removed with rotary evaporator. The yield was 1.6 g (80%) of expected D3TD$_{m-1}$M polymer and MD$_m$M(dicapped) by-product polymer. Structure of synthesized molecules was validated by ^{29}Si NMR spectroscopy and accurate mass measurements (see Supplementary Information).

2.4. Nuclear magnetic resonance

Synthesized authentic compounds, as well as plasma polymerized thin films (first scrapped from the glass substrates and ground to a fine powder), were placed in a zirconium dioxide rotor of 4-mm outer diameter for NMR analysis (Bruker Avance III 400 MHz WB Solid State spectrometer). Quantitative single pulse magic angle spinning (SPMAS) and cross polarization magic angle spinning (CPMAS) NMR spectra were obtained at the ^{29}Si resonance frequency of 79.5 MHz. For quantitative ^{29}Si SPMAS experiments, typical acquisition parameters included 4.5 μs 90° pulse, 225 s recycle delays (equal to five times the longest relaxation time), 512 scans and spin rate of 7 kHz. For ^{29}Si CPMAS experiments, typical parameters were 8 ms contact time, 5 s recycle delays, 6144 scans, and spin rate of 10 kHz. A ramped ^{1}H pulse was used to circumvent Hartman–Hahn mismatches [20]. To improve the resolution, a dipolar decoupling GT8 pulse sequence [21] was applied during the acquisition time. Liquid samples were directly analyzed by the same Bruker Avance III 400 MHz WB Solid State spectrometer, to eliminate the ^{29}Si NMR glass tube background. About 15 μL of samples were placed in a 4 mm HRMAS zirconium dioxide rotor equipped with Teflon insert to seal the samples in the active volume of the probe. ^{29}Si SPMAS experiment was performed with ^{1}H waltz-16 decoupling pulse sequence during the acquisition time at a spinning rate of 1 kHz. All experiments were performed at ambient temperature. Chemical shifts were referenced to tetramethylsilane, whose resonance was set to 0 ppm. Line fitting of the NMR spectra was performed using Gaussian peaks with DMFIT software package [22]. Assignment of ^{29}Si NMR signals was performed according to values referenced in the literature [23,24].

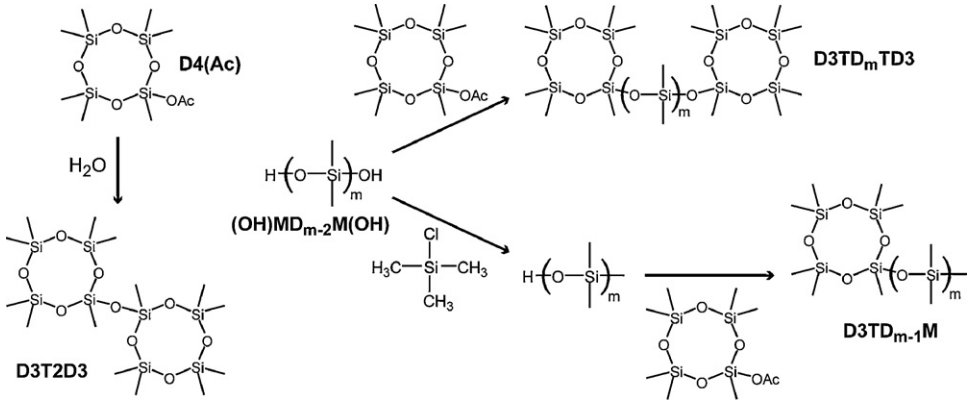

Scheme 1. Synthesis and structure of authentic compounds.

2.5. Mass spectrometry

High resolution MS and MS/MS experiments were performed using a QStar Elite mass spectrometer (Applied Biosystems SCIEX, Concord, ON, Canada) equipped with an electrospray ionization source operated in the positive mode. The capillary voltage was set at +5500 V and the cone voltage at +50 V. In this hybrid instrument, ions were measured using an orthogonal acceleration time-of-flight (oa-TOF) mass analyzer. A quadrupole was used for selection of precursor ions to be further submitted to collision-induced dissociation (CID) in MS/MS experiments. In MS, accurate mass measurements were performed using two reference ions from a poly(ethylene glycol) internal standard, according to a procedure described elsewhere [25]. The precursor ion was used as the reference for accurate measurements of product ions in MS/MS spectra. MS^3 experiments were performed using a 3200 Q-TRAP mass spectrometer (Applied Biosystems SCIEX), equipped with an electrospray ionization source operated in the positive mode. The capillary voltage was set at +5500 V and the cone voltage at +50 V. Primary precursor ions generated in the ion source were selected in the quadrupole analyzer and submitted to CID in a collision cell. Secondary precursor ions produced during collisions were selected and then fragmented in a linear ion trap. In both instruments, air was used as the nebulizing gas (10 psi) while nitrogen was used as the curtain gas (20 psi) as well as the collision gas. Collision energy was set according to the experiments. Instrument control, data acquisition and data processing of all experiments were achieved using Analyst software (QS 2.0 and 1.4.1 for the QqTOF and the QqTrap instruments, respectively) provided by Applied Biosystems.

Plasma polymerized thin films were first scrapped from the glass substrates and ground with a mortar and a pestle to a fine powder. The powder was then solubilized in THF, the solution sonicated for 15 min and centrifugated to separate the insoluble deposit. The clear THF solution was then diluted into a methanolic solution of ammonium acetate (3 mM) to a final 10 $\mu g\,mL^{-1}$ concentration. The synthesized polymers were directly dissolved in THF and further diluted to the same 10 $\mu g\,mL^{-1}$ concentration into methanolic salt solution. Sample solutions were introduced in the ionization source at a 5 $\mu L\,min^{-1}$ flow rate using a syringe pump.

3. Results and discussion

3.1. ESI-MS analysis of the plasma polymer sample

The film obtained upon plasma polymerization of D4 could be partially solubilized in tetrahydrofuran. Comparison of NMR data obtained for the solid film and for the THF extract (Supplementary Fig. S2) indicates that the soluble part of ppD4 (about 25% (w/w) of the whole sample) is mostly composed of the least branched species, consistently with the decreasing solubility of such polymers as their cross-linking degree increases. Indeed, as compared to NMR results obtained for the whole sample (Supplementary Fig. S2a), no signal was observed at around −110 ppm (as typically expected for Si when linked to four oxygen atoms), and species containing Si atoms linked to three oxygen atoms, characterized by a signal at about −66 ppm, were found of relative lower abundance in the THF extract (Supplementary Fig. S2b). The mass spectrum obtained after electrospray ionization of the THF extract is dominated by a peak at *m/z* 596, the ammonium adduct of a 578 Da compound also observed as a protonated molecule at *m/z* 579 (Fig. 1).

Apart from this signal, multiple distributions of even *m/z* ions are observed, confirming species are mainly ionized as ammonium adducts. The 282 Da repeat unit evidenced in the major peak series, starting from *m/z* 596, could also be found in secondary distributions. Since a 74 Da shift (typically the mass of a DMS unit) was systematically measured between the different series, all ions observed in Fig. 1 were envisaged as cationized co-oligomers and hence associated with a (*n*; *m*) couple to indicate their co-monomeric composition. Based on the structure of the D4 reagent, accurate mass measurements of co-oligomer adducts allowed their elemental composition to be determined (Supplementary Table S1) and a general structure to be proposed for the detected co-polymer, as shown in the inset of Fig. 1. According to the nomenclature used for silicon-containing compounds, respectively naming Si atoms as

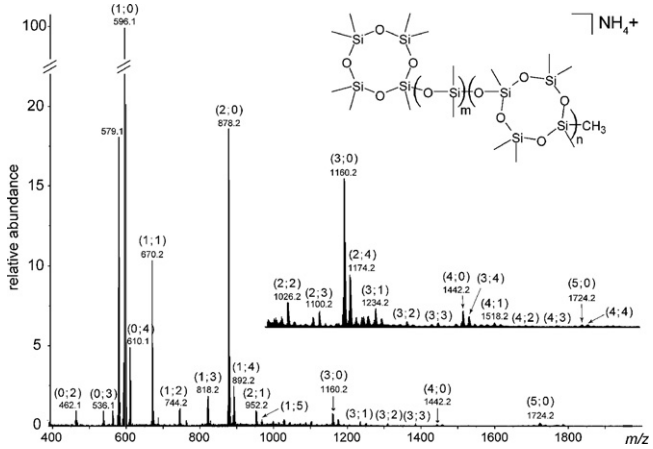

Fig. 1. ESI mass spectrum of the THF-soluble part of the plasma polymer film, further diluted with a methanolic solution of ammonium acetate (3 mM). Peaks are annotated with their co-monomeric (*n*; *m*) composition according to the proposed structure. Inset: zoom of the mass spectrum on the *m/z* 1000–2000 range.

M, D, T and Q when linked to 1–4 oxygen atoms, each molecule in the plasma–polymer sample would then contain *n*TD2T units and *m*D units, as well as a D3T α-end group and a methyl ω termination. In other words, plasma polymerization of D4 would have produced cyclolinear polysiloxanes, in which cyclic units composed of four DMS are covalently connected by linear DMS segments.

Due to the lack of established dissociation rules to understand MS/MS data obtained for these co-oligomeric species, some authentic compounds were synthesized to validate the proposed structures. In this context, the major compound electrosprayed from the soluble part of the plama polymer and assigned to (1; 0) was first studied. Then, co-oligomers were considered as different series of oligomers with a constant *n* or *m* number of co-monomers.

3.2. Major compound (m = 578 Da)

Detected as an ammonium adduct (*m/z* 596) and as a protonated molecule (*m/z* 579) in the ESI mass spectrum of Fig. 1, this compound is proposed to be D3T2D3. It has been synthesized as summarized in the left-hand part of Scheme 1, accurately mass measured (Supplementary Fig. S3) and structurally validated by ^{29}Si NMR (Supplementary Fig. S4). In particular, the NMR integrals measured for D (at −20.8 ppm) and T (at −67.2 ppm) signals were respectively 3.4 and 1.0 (Supplementary Fig. S4), which is consistent with a D3T2D3 compound containing six cyclic D and two T units. Collisional activation of the protonated D3T2D3 (Fig. 2) produced by electrospray gave rise to the same MS/MS data as those obtained upon CID of the *m/z* 579 ion generated from the plasma-polymer sample, validating the structure proposed for this major compound.

All mechanisms proposed to account for the formation of product ions observed in this CID spectrum (accurately mass measured as reported in Supplementary Table S2) are presented in Scheme 2. As depicted by the pathway with plain arrows, a 1,3-methyl transfer concerted with protonation of an oxygen atom would first occur in the precursor ion, allowing the opening of the cyclic monomer into a linear chain containing three DMS units. A 1,4- or 1,6-backbiting mechanism from an oxygen of the chain onto the positively charged Si would respectively produce the *m/z* 147 and *m/z* 73 product ions. Alternatively, elimination of methane from *m/z* 579, involving a methyl group from the cyclic D3T moiety and proton from the hydroxyl group, would allow the formation of the *m/z* 563 product ion. A 1,6-backbiting process concerted with a methyl transfer, either onto or from the terminal trimethylsilyl group, would then lead to the loss of tetramethylsilane (88 Da) and formation of *m/z* 475, or elimination of a 222 Da D3 molecule (previously shown to be a favored reaction [26,27]) and production of *m/z* 341, respectively. A similar process occurring in a 1,4-mechanism would generate *m/z* 401 after the release of a 162 Da neutral. The proposed MS/MS filiations were supported by MS^3 experiments, which showed that *m/z* 475, *m/z* 401 and *m/z* 341 could only be generated upon dissociation of the *m/z* 563 product ion (Supplementary Fig. S5). In particular, pathways such as *m/z* 579 → *m/z* 475 → *m/z* 401 and *m/z* 579 → *m/z* 401 → *m/z* 341 could be excluded based on MS^3 data (Supplementary Fig. S5). Protonation of an oxygen atom in the *m/z* 579 precursor ion could also occur prior to any methyl transfer, allowing one of the D3T ring to be opened. If protonation occurs as depicted with a dotted arrow in Scheme 2, a cyclic 224 Da neutral could be released upon a 1,7-methyl transfer, accounting for the formation of *m/z* 355. Alternatively, upon oxygen protonation according to the plain arrow, the charged silicon will be located in the end-group of the PDMS chain and further transfer of a methyl group would account for the formation of the *m/z* 221 product ion. Finally, protonation of the oxygen bridge between the two D3T moieties (Scheme 2, bold arrow) would generate a fragment detected at *m/z* 281.

The compound yielding the main signal in the ESI-MS spectrum of the ppD4 soluble part would actually be D3T2D3, that is, a molecule resulting from association of two D4 monomers *via* an oxygen bridge. This result is consistent with NMR data, showing that the NMR spectrum obtained for the THF extract (Supplementary Fig. S2b) is very similar to that of the authentic D3T2D3 molecule (Supplementary Fig. S4), with signals of cyclic D and T respectively observed at −20.8 and −68.1 ppm with integrals measured in a ratio of about 3:1. This finding also supports our preliminary assumption regarding stability of the D4 monomer, most cyclic features remaining intact during the plasma polymerization process.

3.3. Oligomers with m = 0

This distribution would actually consist of a homopolymer of TD2T, bearing a D3T α-end group and a methyl ω termination, and should hence be called D3T(TD2T)$_n$TD3. Since no synthesis protocol could be found in the literature to prepare such molecules, MS/MS data obtained for ammonium adducts of plasma oligomers were studied with regards to the dissociation behavior of D3T2D3, which is actually the first congener of this series. As illustrated in Fig. 3 for *n* = 3–5 (associated accurate mass measurements can be found in Supplementary Table S3), precursor ions would first eliminate ammonia to generate protonated molecules, considered as the actual dissociating species.

A distribution of product ions starting from *m/z* 281 and spaced by 282 Da (annotated by filled circles in Fig. 3) could be explained according to the same reaction depicted in Scheme 2 for the formation of *m/z* 281 from [D3T2D3+H]$^+$. These product ions are detected at *m/z* values equal to 281 + 282*i*, *i* ranging from 0 to (*n* − 1), with *n* the number of monomers in the precursor ion, that is, the number of oxygen bridges to be protonated between two D3T cycles. Alternatively, protonated oligomers were observed to eliminate a methane molecule, followed by the release of a 222 Da neutral. Such a consecutive dissociation was validated by MS^3 experiments and would proceed as previously depicted for D3T2D3 in Scheme 2. A similar 222 Da loss could also be envisaged to occur from each product ion at *m/z* 281 + 282*i*, after a set of three successive methyl transfers has occurred, as illustrated in Scheme 3 (upper part) to account for the *m/z* 563 → *m/z* 341 pathway. All product ions arising from a 222 Da neutral loss are annotated with open circles in Fig. 3. The mechanism described in Scheme 2 with a dotted arrow would also proceed from [D3T(TD2T)$_n$TD3+H]$^+$ to form a *m/z* 355 + 282*i* product ion series, starting from the abundant *m/z* 355 fragment but observed with rapidly decreasing intensity as their size increases (as annotated with stars in Fig. 3). As the precursor ion size increases, numerous other ion series spaced by 282 Da are observed, with most abundant congeners in the low *m/z* range of the CID spectrum. All these ion series could be accounted for by applying one or the other mechanisms previously described in Scheme 2. For example, a methyl transfer concerted with protonation of an oxygen atom (as previously depicted in Scheme 2 with plain arrows) followed by a 1,4-backbitting mechanism would generate product ions at *m/z* 147, *m/z* 429, and *m/z* 711 when the methyl transfer has respectively proceeded in *n*th, (*n* − 1)th, (*n* − 2)th monomer. This pathway is illustrated in Scheme 3 (lower part) for the formation of *m/z* 711. These product ions (annotated by filled triangles in Fig. 3b and c) could further rearrange upon various methyl transfers, ultimately leading to product ions annotated with open triangles upon a 222 Da neutral loss (Scheme 3).

In summary, based on dissociation reactions proposed to occur from the protonated authentic D3T2D3, ions assigned to co-oligomer adducts with *m* = 0 in the ESI mass spectrum of the plasma-polymer sample could well be of the form D3T(TD2T)$_n$TD3.

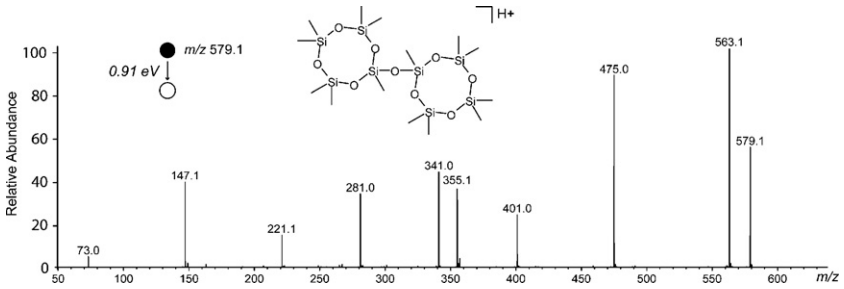

Fig. 2. CID spectrum of the *m/z* 579 precursor ion obtained upon electrospray ionization of the synthesized authentic D3T2D3 compound (center-of-mass collision energy: 0.91 eV).

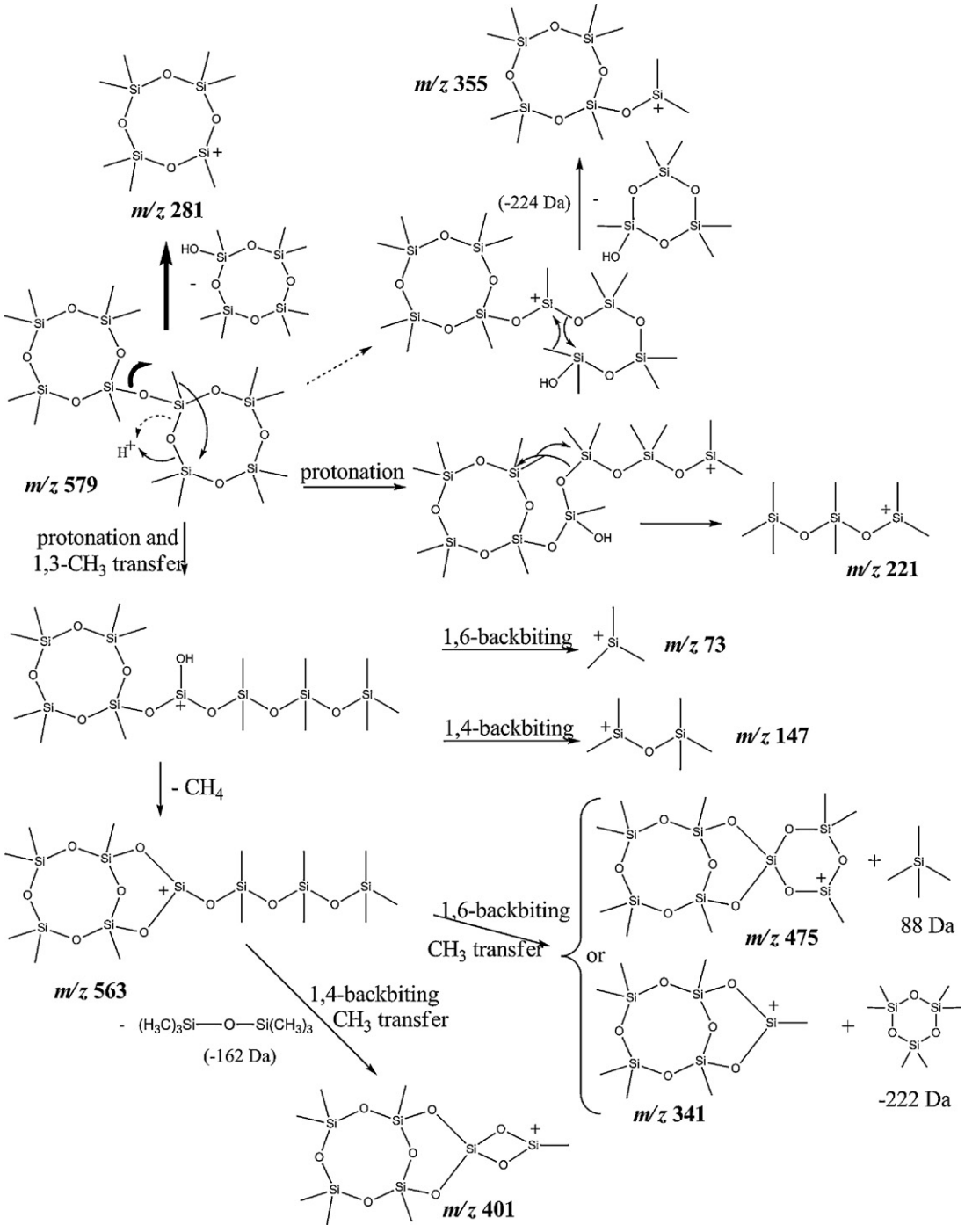

Scheme 2. Proposed reactions for dissociation of $[D3T2D3+H]^+$ at *m/z* 579.

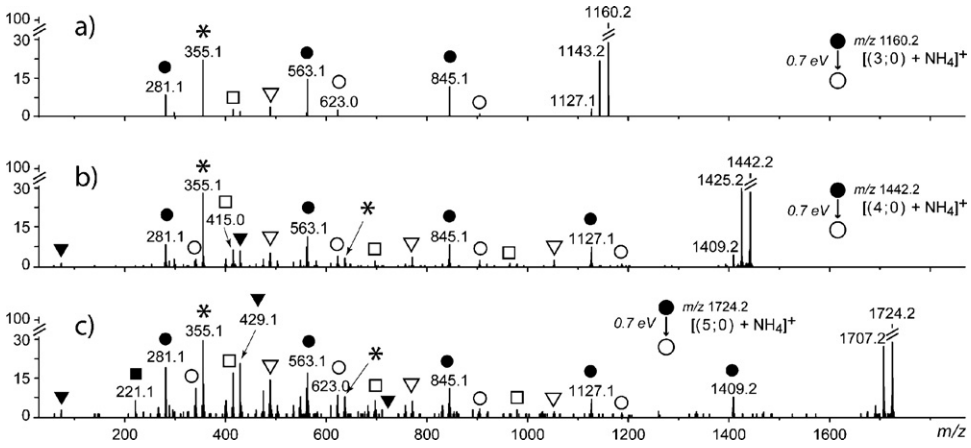

Fig. 3. CID spectra of ammonium adducts of proposed D3T(TD2T)$_n$TD3 oligomers with (a) $n = 3$ at m/z 1160, (b) $n = 4$ at m/z 1442, and (c) $n = 5$ at m/z 1724, using a collision energy of 0.7 eV (center-of-mass frame).

However, MS/MS patterns usually observed for linear PDMS exhibits peaks only in the low m/z range of the CID spectra due to fast dissociation of primary product ions [26,27]. Therefore, detection of fragments of high m/z values in CID spectra of Fig. 3 strongly suggests that precursor ions selected here for dissociation are not only linear oligomers but also isomers of different branching degree, in which branching groups would prevent elimination of usually released neutrals.

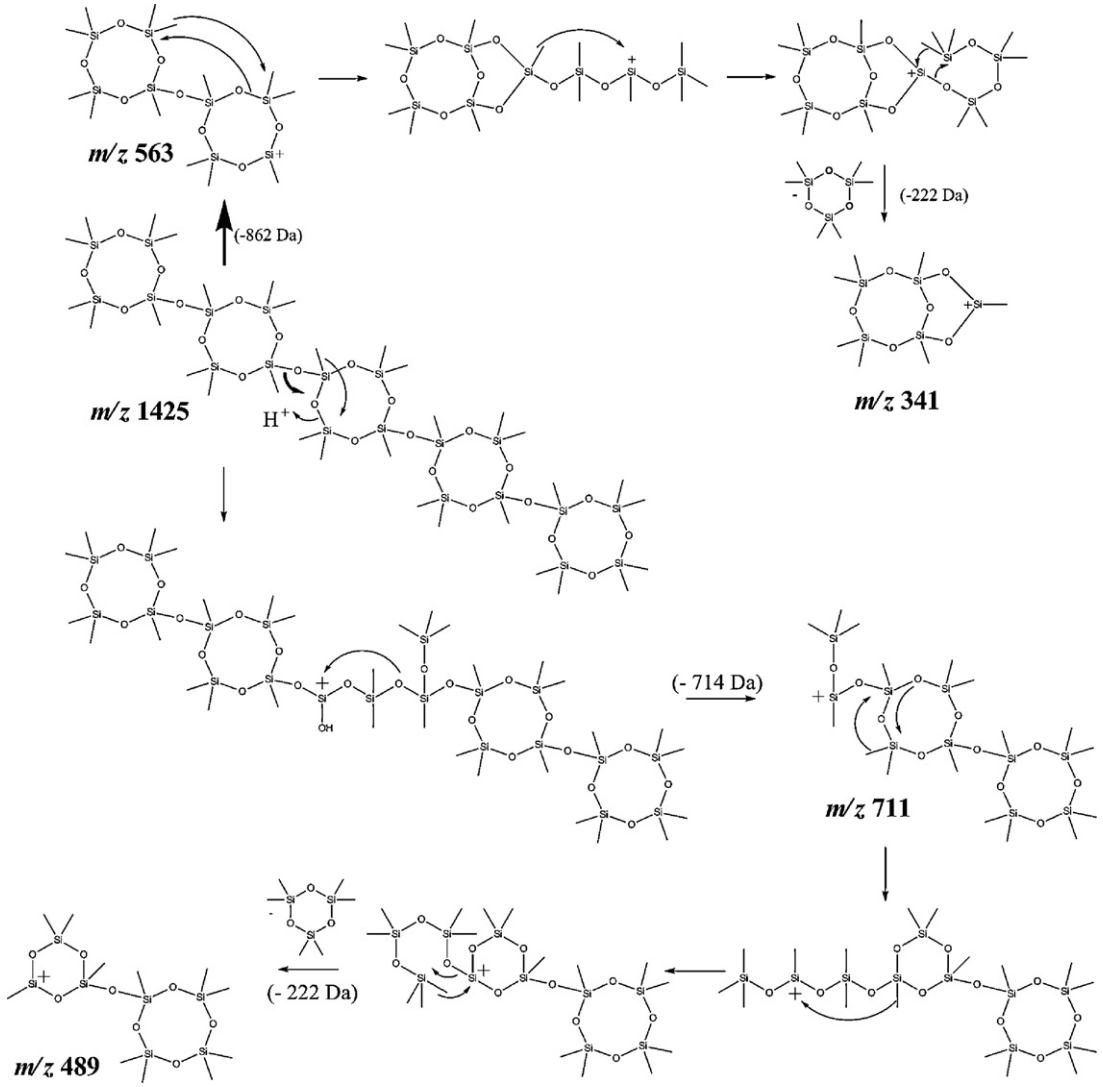

Scheme 3. Proposed mechanisms to account for the formation of m/z 563 and m/z 711 primary product ions from [D3T(TD2T)$_4$TD3+H]$^+$ at m/z 1425, both further releasing a 222 Da neutral to generate secondary fragments.

3.4. Oligomers with n = 0

This small ion distribution, with m ranging from 2 to 6, would be a PDMS homopolymer with a D3T α initiating group. Since the nature of the end-groups is known to strongly affect the dissociation behavior of PDMS [13], CID of these ammonium adducts was compared to that of authentic D3TD$_{m-1}$M molecules, synthesized as shown in the lower right-hand part of Scheme 1. Structure of this polymer standard (which sample also contains MD$_m$M as a synthetic side-product) was validated by ^{29}Si NMR and accurate mass measurements, as reported in Supplementary Figs. S6–S7 and Table S4. More specifically, D3TD$_{m-1}$M oligomers were clearly evidenced by signals at −21.1 ppm (cyclic D) and −67.1 ppm (cyclic T) while MD$_m$M molecules were characterized by signals at +5.4 ppm (M) and −23.7 ppm (linear T). CID data obtained for authentic D3TD$_m$M oligomers with m = 1, 3 and 5 (Fig. 4, left) could be rationalized based on dissociation reactions previously described for [D3T2D3+H]$^+$, all proposed pathways in the following being supported by accurate mass data presented in Supplementary Table S5. Protonated molecules formed upon elimination of ammonia from the precursor ion are observed to release methane. In the case of D3TDM oligomer (Fig. 4a, left-hand part), loss of methane would be followed by a methyl transfer to the Si atom in the last DMS monomer, allowing the elimination of tetramethylsilane to produce m/z 341. For upper congeners, protonation of oxygen atoms in the linear PDMS chain, followed by a Si—O bond cleavage to allow the release of a neutral containing the ω end-group, would generate a first product ion series, detected at m/z values such as 281 + 74j, with j designating the position number of the protonated oxygen and hence, the number of linear DMS units linked to the α end-group in these so-called α_j products ions. Consistently with the dissociation behavior reported for linear PDMS [26,27], only α_{0-3} were detected with high abundance despite increasing the size of the linear PDMS segment in the precursor ion (Fig. 4c, left-hand part). Formation of products ions with a positively charged terminal Si atom is indeed rapidly followed by the release of a very stable three DMS cyclic species (222 Da) in a backbiting process to produce α_{j-3} species. Alternatively, as also evidenced in MS^3 experiments, α_j ions were shown to eliminate tetramethylsilane (88 Da), accounting for the product ions at m/z 267, m/z 341 and m/z 415 observed with a low abundance in Fig. 4b and c. A last product ion series (annotated with stars in Fig. 4) would arise from the same mechanism as described above for the formation of α_j ions but with a Si—O bond cleavage yielding neutrals containing the α termination. It should be noted here that dissociation of these linear PDMS oligomers greatly contrasts with that of trimethylsilyl-terminated PDMS, shown to mainly generate three major product ions at m/z 221, m/z 295 and m/z 369 regardless of the precursor ion size [26], illustrating the strong influence of terminating moieties on MS/MS data obtained for PDMS, as already reported in the literature [13,27–30].

Comparison of MS/MS spectra obtained for D3TD$_{m-1}$M authentic standards and for species of the same elemental composition in the plasma-polymer sample shows that product ions are detected at the same m/z values. However, apart from the case with m = 1 where very similar MS/MS patterns were obtained (Fig. 4a), CID data are very dissimilar when produced from synthesized *vs* plasma polymerized species (Fig. 4b and 4c). These discrepancies are however mainly due to peak relative intensities. For example, relative abundance of protonated molecules formed after release of ammonia from m/z 610 precursor ions (Fig. 4b) clearly indicates a different stability for m/z 593 depending on the origin of the dissociating adduct.

This result would suggest that, in contrast to the linear DMS chain in the synthesized molecules, plasma produced oligomers would contain a segment with branching DMS units enabling a stronger proton binding due to the proximity of multiple oxygen sites. Similarly, product ions belonging to minor series when formed from dissociation of authentic standards are observed as major fragments of plasma polymer precursor ions (*e.g.*, m/z 341 and m/z 443 in Fig. 4c). However, a more detailed structural analysis based on such MS/MS data remains highly hypothetical due to the probable co-existence of multiple positional isomers in the plasma polymer.

3.5. Co-oligomers with n = 1

Congeners of this series can be seen as oligomers of a linear PDMS with D3T as the α end-group and TD3 as the ω termination. Such a D3TD$_m$TD3 polymer could be synthesized (as shown in the upper right-hand part of Scheme 1) and its ESI mass spectrum displayed a distribution of singly charged oligomer adducts spaced by 74 Da and with m ranging from 1 to 15 (Supplementary Fig. S8). Structure and elemental composition of these standard oligomers were respectively supported by ^{29}Si NMR (Supplementary Fig. S9) and accurate mass measurements (Supplementary Table S6). As expected, integrals of NMR signals at −21.1 ppm (cyclic D) and −67.1 ppm (cyclic T) were measured in a ratio of about 3:1. Interestingly, an average m value of 10 in D3TD$_m$TD3 could be calculated from the integral ratio between the linear D signal (at −23.7 ppm) and the signal assigned to cyclic T (at −67.1 ppm), indicating that ESI-MS data were affected by a quite strong bias towards low mass (Supplementary Fig. S8). CID data obtained for authentic oligomers with m = 2, 4 and 6 (Fig. 5, upper part) could readily be rationalized by combining dissociation reactions previously described for [D3T2D3+H]$^+$ and for [D3TD$_{m-1}$M+H]$^+$.

The same annotation as used in Fig. 4 could hence be applied and these assignments were supported by accurate mass measurements (Supplementary Table S7). For example, once the dissociating ammonium adduct at m/z 744 has eliminated ammonia, protonated D3TD$_2$TD3 at m/z 727 is observed to eliminate CH_4, yielding the m/z 711 product ion (Fig. 5a, upper part). This m/z 711 ion would further release a 162 Da or a 222 Da neutral (as supporting by MS^3 experiments and according to mechanisms shown in Scheme 2) to form m/z 549 and m/z 489 fragments, respectively. Protonation of oxygen atoms in the linear PDMS segment of D3TD$_m$TD3 followed by a Si—O bond cleavage would generate the previously defined α_j product ion series, whatever the cleaved Si—O(H$^+$) bond due to the symmetry of the studied oligomers. As a consequence of rapid dissociation of largest α_j ions, D3TD$_m$TD3 congeners with m > 6 all exhibit the same MS/MS spectrum as that shown in the upper part of Fig. 5c.

Comparing these CID data with MS/MS spectra obtained for corresponding species in the plasma-polymer sample (Fig. 5, lower part) first shows that the same product ions are formed in both cases. Computing the similarity between two MS/MS spectra [31], high correlation coefficients were found to indicate a good agreement between CID data of synthesized standards and plasma polymer species, as long as the size of the precursor ions remains quite low. For example, R^2 values of 0.973 and 0.988 were respectively calculated for the cases of D3TD$_2$TD3 (Fig. 5a) and D3TD$_3$TD3 (data not shown). However, discrepancies between MS/MS of authentic compounds and plasma-polymer species are observed to increase with the size of the precursor ion. For example, calculated R^2 values were respectively of 0.967 and 0.933 for data presented in Fig. 5b and c. The evolution of the R^2 correlation coefficient as a function of m in D3TD$_m$TD3 is further detailed in Supplementary Fig. S10. The main spectral difference which accounts for the observed decreasing correlation between upper and lower spectra in Fig. 5 is the presence of the whole series of abundant α_j products ions in CID of plasma–polymer species, as observed with j ranging from 0 to m in Fig. 5b and c. This result

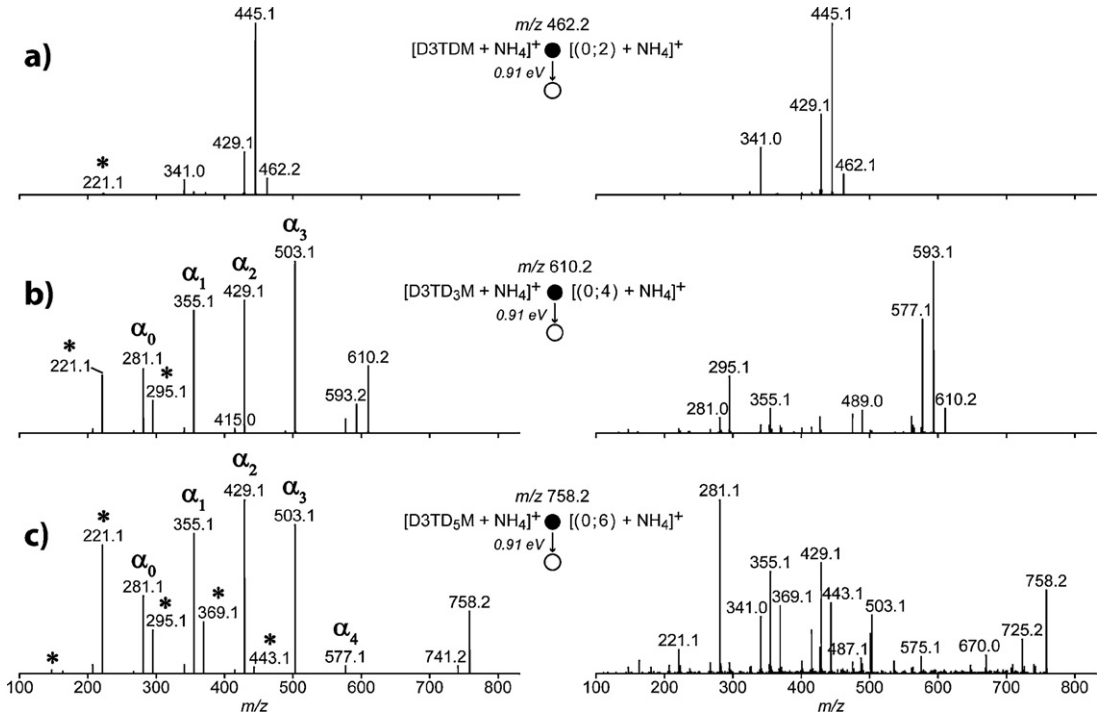

Fig. 4. CID spectra of ammonium adducts at (a) *m/z* 462, (b) *m/z* 610 and (c) *m/z* 758 formed after electrospray ionization of the synthesized D3TD$_{m-1}$M (left-hand part) and of the plasma–polymer sample (right-hand part), using a 0.91 eV collision energy (center-of-mass frame).

strongly suggests the presence of isomers in the plasma-polymer species, with the *m* DMS units arranged as a branched chain rather than as a linear segment. As a result, protonation of an O atom in the DMS segment would conduct to product ions in which branching groups would prevent the release of the stable 222 Da cyclic D3 from some of the largest α_j products ions to generate α_{j-3} congeners, usually observed to strongly deplete the signal of ions with a long linear DMS chain [26,27]. Alternatively, some compounds with two cyclic units within the polymer skeleton rather than as terminating groups may also be envisaged.

3.6. Co-oligomers (n; m)

The dissociation behavior established for particular species (*n*; *m* = 0) and (*n* = 1; *m*) was then used to understand CID spectra of typical (*n*; *m*) co-oligomers, for which no authentic compound could be synthesized. The number of product ions arising from dissociation of co-oligomers (particularly random ones) is usually expected to be larger than for homopolymers of their constituting units, giving rise to complex CID spectra [12]. Surprisingly, MS/MS data obtained for ammonium adducts of the studied co-oligomers were quite simple, as shown with the example of the molecule with *m* = 4 and *n* = 4 in Fig. 6.

All product ions in this MS/MS spectrum could be accounted for by considering different arrangements of co-monomers within the precursor ions. Once the activated ammonium adducts have eliminated ammonia, location of the proton on different oxygen atoms in the so-formed protonated molecules would induce the cleavage of the O(H$^+$)—Si bond (as described for the formation of *m/z* 281 in Scheme 2), generating the main product ion series. These fragments would all contain the initiating cyclic α moiety and were annotated $\alpha_{i;j}$ in Fig. 6, with *i* and *j* respectively indicating the number of cyclic and linear units they contain. For example, product ion $\alpha_{0;4}$ at *m/z* 577 would consist of four DMS units linked to the

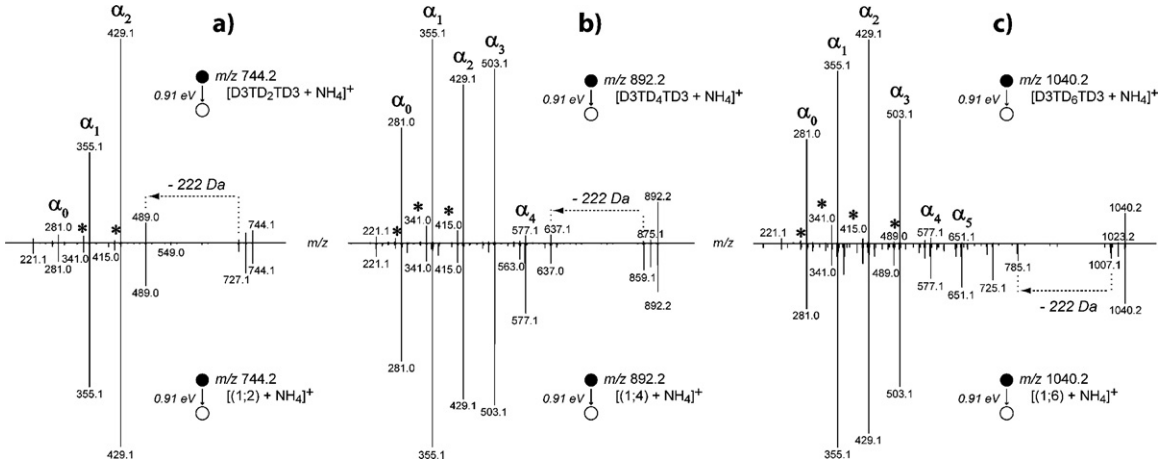

Fig. 5. CID spectra of precursor ions at (a) *m/z* 744, (b) *m/z* 892 and (c) *m/z* 1040 formed after electrospray ionization of the synthesized D3TD$_m$TD3 (upper part) and of the plasma–polymer sample (lower part).

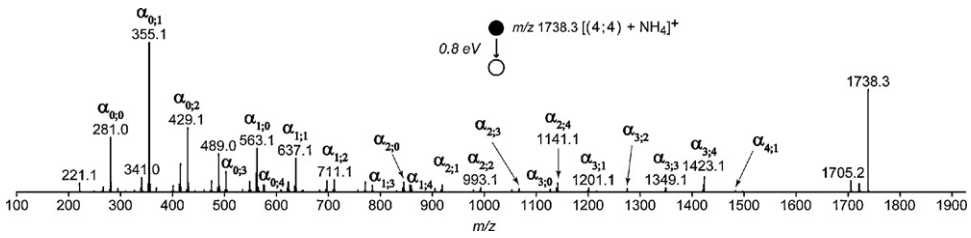

Fig. 6. CID spectrum of *m/z* 1738, assigned to the ammonium adduct of co-oligomer (4; 4), at a 0.8 eV collision energy (center-of-mass frame).

α end-group, indicating that the activated *m/z* 1738 precursor ion would actually be the ammonium adduct of a block co-oligomer such as $D3TD_4(TD2T)_3TD3$. In contrast, detection of $\alpha_{4;1}$ at *m/z* 1483 would suggest a $D3T(TD2T)_4D_3M$ structure for the precursor ion, that is, also a block co-oligomer but with DMS units linked to the ω end-group. Moreover, detection of $\alpha_{i;j}$ with nearly all possible *i*; *j* combinations would be in favor of random co-oligomers. It should also be noted that different reactions can give rise to the same fragments, as for example the *m/z* 1483 product ion assigned to $\alpha_{4;1}$ but which could also be generated upon release of a 222 Da neutral from *m/z* 1705, formed after the protonated co-oligomer has eliminated methane. In addition, most product ions observed in Fig. 6 could also be explained as secondary fragments produced during a variety of reactions (*vide supra*), accounting for larger abundance measured for product ions in the low *m/z* range of the CID spectrum. More exhaustive peak assignments are presented with product ion accurate mass measurements in Supplementary Table S8. Finally, as previously discussed for particular species (*n*; *m* = 0) and (*n* = 1; *m*), the existence of co-oligomers with branching units has to be envisaged to account for the unexpected stability of high *m/z* product ions.

4. Conclusion

Structural study of the THF soluble part of the ppD4 film using tandem mass spectrometry has revealed a random copolymer constituted of four DMS-containing cyclic units and linear DMS segments. Discrepancies observed between MS/MS data of these co-oligomer ammonium adducts with CID spectra obtained from electrosprayed authentic compounds strongly suggests the presence of branched units in plasma polymerized species. However, due to the lack of appropriate standards to establish the dissociation behavior of branched species, structural conclusions drawn from MS/MS (as well as MS^n) data would be highly speculative. From a mechanistic point of view, these results show that some cyclic monomers remain intact during the plasma polymerization process while others would be opened into linear DMS chains, most probably in a radical mechanism. Further decomposition and/or reactions of the latter species with cyclic precursors would account for the presence of cyclolinear polysiloxanes with different linear DMS units. Alternatively, opening of four DMS-containing cycles could also occur within the $D3T(TD2T)_nTD3$ homopolymer. Indeed, a closer inspection of the ESI mass spectrum of the THF extract shown in Fig. 1 indicates that those co-oligomers with *m* = 4 DMS units are systematically of higher abundance than their (*n*; 3) and (*n*; 5) congeners. For example, the peak at *m/z* 892 assigned to the ammonium adduct of (1; 4) is more intense than $[(1; 3)+NH_4]^+$ and $[(1;5)+NH_4]^+$, respectively observed at *m/z* 818 and *m/z* 966. This cycle opening in monomers of $D3T(TD2T)_nTD3$ would hence give rise to linear segments of three DMS units branched with a fourth one. Presence of multiple positional isomers is also strongly suspected in the studied sample, preventing any more precise molecular description in this extract. In order to find out whether these structural findings could be used as a basis to describe the whole ppD4 film, methodologies aimed at specifically breaking cross-linking bonds in a controlled manner are currently investigated to enable electrospray mass spectrometric analysis of the major insoluble ppD4 part.

Acknowledgments

L. Charles acknowledges support from Spectropole, the Analytical Facility of Aix-Marseille University, by allowing a special access to the instruments purchased with European Funding (FEDER OBJ2142-3341). Financial support by the Luxembourg Research Funding Association FNR (Fond National de la Recherche) is also gratefully acknowledged. The authors also acknowledge Dr. Mertz for the ellipsometric thickness measurement of the plasma polymer films deposited on silicon substrate

Appendix A. Supplementary data

Supplementary data associated with this article can be found, in the online version, at doi:10.1016/j.ijms.2012.01.007.

References

[1] H. Biederman, Plasma Polymer Films, Imperial College Press, Covent Garden, UK, 2004.
[2] Y. Leterrier, Durability of nanosized oxygen-barrier coatings on polymers – internal stresses, Prog. Mater. Sci. 48 (2003) 1–55.
[3] L. O'Neill, L.A. O'Hare, S.R. Leadley, A.J. Goodwin, Atmospheric pressure plasma liquid deposition – a novel route to barrier coatings, Chem. Vap. Deposition 11 (2005) 477–479.
[4] M. Creatore, F. Palumbo, R. d'Agostino, P. Fayet, RF plasma deposition of SiO_2-like films: plasma phase diagnostics and gas barrier film properties optimisation, Surf. Coat. Technol. 142 (2001) 163–168.
[5] J. Bardon, J. Bour, H. Aubriet, D. Ruch, B. Verheyde, R. Dams, S. Paulussen, R. Rego, D. Vangeneugden, Deposition of organosilicon-based anticorrosion layers on galvanized steel by atmospheric pressure dielectric barrier discharge plasma, Plasma Processes Polym. 4 (2007) S445–S449.
[6] J. Bour, J. Bardon, H. Aubriet, D. Del Frari, B. Verheyde, R. Dams, D. Vangeneugden, D. Ruch, Different ways to plasma-polymerize HMDSO in DBD configuration at atmospheric pressure for corrosion protection, Plasma Processes Polym. 5 (2008) 788–796.
[7] C. Tendero, C. Tixier, P. Tristant, J. Desmaison, P. Leprince, Atmospheric pressure plasmas: a review, Spectrochim. Acta, Part B 61 (2006) 2–30.
[8] V. Rouessac, S. Roualdes, J. Durand, In situ mass spectrometry analyses of the fragmentation of linear and cyclic siloxanes in a glow discharge compared with ex situ FTIR analyses of the deposits, Chem. Vap. Deposition 8 (2002) 155–161.
[9] V. Barranco, P. Thiemann, H.K. Yasuda, M. Stratmann, G. Grundmeier, Spectroscopic and electrochemical characterisation of thin cathodic plasma polymer films on iron, Appl. Surf. Sci. 229 (2004) 87–96.
[10] P. Raynaud, B. Despax, Y. Segui, H. Caquineau, FTIR plasma phase analysis of hexamethyidisiloxane discharge in microwave multipolar plasma at different electrical powers, Plasma Processes Polym. 2 (2005) 45–52.
[11] F. Massines, N. Gherardi, A. Fornelli, S. Martin, Atmospheric pressure plasma deposition of thin films by townsend dielectric barrier discharge, Surf. Coat. Technol. 200 (2005) 1855–1861.
[12] M.S. Montaudo, Mass spectra of copolymers, Mass Spectrom. Rev. 21 (2002) 108–144.
[13] C. Wesdemiotis, N. Solak, M.J. Polce, D.E. Dabney, K. Chaicharoen, B.C. Katzenmeyer, Fragmentation pathways of polymer ions, Mass Spectrom. Rev. 30 (2011) 523–559.
[14] T.S. Radhakrishnan, New method for evaluation of kinetic parameters and mechanism of degradation from pyrolysis-GC studies: thermal degradation of polydimethylsiloxanes, J. Appl. Polym. Sci. 73 (1999) 441–450.

[15] G. Deshpande, M.E. Rezac, The effect of phenyl content on the degradation of poly(dimethyl diphenyl) siloxane copolymers, Polym. Degrad. Stab. 74 (2001) 363–370.
[16] S.M. Lomakin, E.V. Koverzanova, N.G. Shilkina, S.V. Usachev, G.E. Zaikov, Thermal degradation of polystyrene–polydimethylsiloxane blends, Russ. J. Appl. Chem. 76 (2003) 472–482.
[17] K. Hayashida, S. Tsuge, H. Ohtani, Flame retardant mechanism of polydimethylsiloxane material containing platinum compound studied by analytical pyrolysis techniques and alkaline hydrolysis gas chromatography, Polymer 44 (2003) 5611–5616.
[18] J. Petersen, R. Bechara, J. Bardon, T. Fouquet, F. Ziarelli, L. Daheron, V. Ball, V. Toniazzo, M. Michel, A. Dinia, D. Ruch, Atmospheric plasma deposition process: a versatile tool for the design of tunable siloxanes-based plasma polymer films, Plasma Processes Polym. 8 (2011) 895–903.
[19] J. Daum, G. Erdodi, J.P. Kennedy, Cyclolinear polysiloxanes. I. synthesis and characterization, J. Polym. Sci. Part A: Polym. Chem. 44 (2006) 4039–4052.
[20] O.B. Peersen, X.L. Wu, I. Kustanovich, S.O. Smith, Variable-amplitude cross-polarization MAS NMR, J. Magn. Reson. Ser. A 104 (1993) 334–339.
[21] G. Gerbaud, F. Ziarelli, S. Caldarelli, Increasing the robustness of heteronuclear decoupling in magic-angle sample spinning solid-state NMR, Chem. Phys. Lett. 377 (2003) 1–5.
[22] D. Massiot, F. Fayon, M. Capron, I. King, S. Le Calve, B. Alonso, J.O. Durand, B. Bujoli, Z.H. Gan, G. Hoatson, Modelling one- and two-dimensional solid-state NMR spectra, Magn. Reson. Chem. 40 (2002) 70–76.
[23] G. Engelhardt, H. Jancke, Structure investigation of organo-silicon polymers by Si-29 NMR, Polym. Bull. 5 (1981) 577–584.
[24] S. Roualdes, R. Berjoan, J. Durand, Si-29 NMR and Si2p XPS correlation in polysiloxane membranes prepared by plasma enhanced chemical vapor deposition, Sep. Purif. Technol. 25 (2001) 391–397.
[25] L. Charles, Influence of internal standard charge state on the accuracy of mass measurements in orthogonal acceleration time-of-flight mass spectrometers, Rapid Commun. Mass Spectrom. 22 (2008) 151–155.
[26] T. Fouquet, S. Humbel, L. Charles, Tandem mass spectrometry of trimethylsilyl-terminated poly(dimethylsiloxane) ammonium adducts generated by electrospray ionization, J. Am. Soc. Mass Spectrom. 22 (2011) 649–658.
[27] T. Fouquet, S. Humbel, L. Charles, Dissociation characteristics of alpha,omega-dihydride poly(dimethylsiloxane) ammonium adducts generated by electrospray ionization, Int. J. Mass Spectrom. 306 (2011) 70–76.
[28] J. Renaud, A.M. Alhazmi, P.M. Mayer, Comparing the fragmentation chemistry of gas-phase adducts of poly(dimethylsiloxane) oligomers with metal and organic ions, Can. J. Chem. 87 (2009) 453–459.
[29] H. Chen, Endgroup-assisted siloxane bond cleavage in the gas phase, J. Am. Soc. Mass Spectrom. 14 (2003) 1039–1048.
[30] A.M. Leigh, P. Wang, M.J. Polce, C. Wesdemiotis, In tandem mass spectrometry of poly(siloxane)s, in: 53rd ASMS Conference on Mass Spectrometry and Allied Topics, June 5–9, San Antonio, Texas, 2005.
[31] I. Beer, E. Barnea, T. Ziv, A. Admon, Improving large-scale proteomics by clustering of mass spectrometry data, Proteomics 4 (2004) 950–960.